Ordered and disordered stealthy hyperuniform point patterns across spatial dimensions

Peter K. Morse [1,2,3,*] Paul J. Steinhardt [2] and Salvatore Torquato [1,2,4,3,5,†]

[1]*Department of Chemistry, Princeton University, Princeton, New Jersey 08544, USA*
[2]*Department of Physics, Princeton University, Princeton, New Jersey 08544, USA*
[3]*Princeton Institute of Materials, Princeton University, Princeton, New Jersey 08544, USA*
[4]*Princeton Center for Theoretical Science, Princeton University, Princeton, New Jersey 08544, USA*
[5]*Program in Applied and Computational Mathematics, Princeton University, Princeton, New Jersey 08544, USA*

(Received 30 April 2024; accepted 7 August 2024; published 6 September 2024)

In previous work [Phys. Rev. X **5**, 021020 (2015)] it was shown that stealthy hyperuniform systems can be regarded as hard spheres in Fourier space in the sense that the structure factor is exactly zero in a spherical region around the origin in analogy with the pair-correlation function of real-space hard spheres. While this earlier work focused on spatial dimensions $d = 1$–4, here we extend the analysis to higher dimensions in order to make connections to high-dimensional sphere packings and the mean-field theory of glasses. We exploit this correspondence to confirm that the densest Fourier-space hard-sphere system is that of a Bravais lattice in contrast to real-space hard spheres, whose densest configuration is conjectured to be disordered. In passing, we give a concise form for the position of the first Bragg peak. We also extend the virial series previously suggested for disordered stealthy hyperuniform systems to higher dimensions in order to predict spatial decorrelation as a function of dimension. This prediction is then borne out by numerical simulations of disordered stealthy hyperuniform ground states in dimensions $d = 2$–8, which have only recently been made possible due to a highly parallelized algorithm.

DOI: 10.1103/PhysRevResearch.6.033260

I. INTRODUCTION

Hyperuniform systems are defined by a structure factor $S(\mathbf{k})$ which approaches zero as the wave number $k \equiv |\mathbf{k}|$ approaches zero, yielding density fluctuations that are anomalously suppressed at long length scales as compared to standard liquids or gases [1]. These systems describe states that are ubiquitous in nature ranging from ordered systems, like crystals and quasicrystals, to disordered systems, like perfect glasses, fermionic point processes, jammed particle packings, quantum states, plasmas, galaxy distributions, and eigenvalues of random matrices [2]. Hyperuniform systems can be classified according to the precise way the structure factor approaches zero, which is useful because different classes have distinctive properties and applications.

Stealthy hyperuniform point patterns are a subclass of hyperuniform states wherein $S(k)$ is precisely zero within an exclusion region $0 < k < K$ for some positive K, which gives these systems novel transport, photonic, and mechanical properties [2]. For instance, using a protocol that transforms these point patterns into a dielectric network, one can create solids with an isotropic complete photonic band gap [3] with no Anderson localization [4–7]. From a theoretical perspective, their defining property suggests an analogy: Up to two particle correlations, stealthy hyperuniform point patterns can be regarded as hard spheres in Fourier space [8] in the sense that the pair-correlation function for hard spheres, $g_2(r)$, has an exclusion region in real space, where $g_2(r)$ is precisely zero for $0 < r \leqslant \sigma$, where r is the distance between particles and σ is the sphere diameter (see Fig. 1 for a comparison).

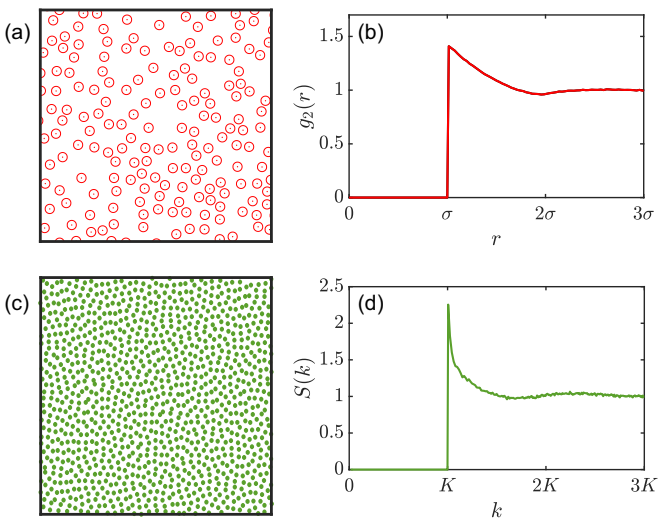

FIG. 1. Comparison between (a) real-space hard disks with (b) their exclusion region in $g_2(r)$ and (c) a disordered stealthy hyperuniform point pattern (Fourier-space hard spheres) with (d) their exclusion region in $S(k)$.

*Contact author: peter.k.morse@gmail.com
†Contact author: torquato@princeton.edu

The analogy breaks down when considering higher-order correlations (g_n with $n > 2$), but the correspondence is strong enough to deduce several properties of stealthy hyperuniform systems. While bearing in mind this qualification, we use the terms stealthy hyperuniform point pattern and Fourier-space hard spheres interchangeably in order to help build intuition regarding their behavior, particularly as the spatial dimension increases.

In considering the analogy, it is natural to extend the concept of packing fraction for hard spheres in real space to Fourier space, as in Ref. [8]. For hard spheres in real space, the packing fraction is proportional to σ^d, where d is the dimension of space. In Fourier space, the effective packing fraction of stealthy hyperuniform configurations is proportional to K^d [8]. In the special case of crystalline stealthy hyperuniform systems, K is simply the location of the first Bragg peak [9], while for disordered stealthy hyperuniform systems, K is the smallest wave number for which $S(K)$ is positive. This suggests a simple question: Is there a direct correspondence between ideal hard-sphere packings in real space and in Fourier space (i.e., solutions to the densest packing, the covering problem, or the quantizer problem [10,11])?

In real space, each of these problems is quite difficult. In particular, the densest packing has only been rigorously proven in dimensions $d = 1$ (a trivial solution), $d = 2$ [12], $d = 3$ [13], $d = 8$ [14], and $d = 24$ [15]. For all other dimensions, only lower [16] and upper bounds [17,18] have been proven, though conjectured but unproven densest packing candidates are often quoted for $d \leqslant 48$ [10]. Most of these candidates are Bravais lattices, though notable exceptions exist in $d = 10$–13 [19], where the densest known packings are m-component crystals derived through binary codes. The question of the densest crystalline hard-sphere packing in real space is thus made more difficult by the existence of infinitely many non-Bravais crystals (such as the honeycomb crystal in $d = 2$ and hexagonal close packing in $d = 3$). To complicate matters further, it has been conjectured that in large enough d, the densest packing should be disordered due to the decorrelation principle [20], which states that as $d \to \infty$ all unconstrained spatial correlations vanish beyond the hard core and all n-particle correlation functions g_n for $n \geqslant 3$ can be inferred from g_2 and the number density. However, two other possibilities have been suggested through thermodynamic arguments, as discussed in Ref. [21].

For Fourier-space hard spheres, the densest packing in any dimension has constraints that do not exist in real space, allowing for stronger restrictions on its properties. In $d = 1$–4, it was proven [8] that the densest Fourier-space hard-sphere packing in is a Bravais lattice, specifically, the dual to the densest Bravais lattice in real space. This statement was then conjectured to hold for higher dimensions, which we address in Sec. III. The densest configuration in Fourier space thus does not necessarily correspond to the densest configuration in real space except in cases where the densest Bravais lattice is self-dual. Here we derive an expression that makes this statement explicit, thus allowing the full phase diagram of stealthy systems to be computed.

We also comment directly on the decorrelation principle as applied to disordered stealthy hyperuniform states. In Ref. [7] we demonstrated the ability to create large disordered stealthy hyperuniform systems to ultrahigh accuracy by adapting their standard generating protocol to double-double precision on GPUs. With ultrahigh-accuracy systems at our disposal, it is then possible to test the decorrelation principle through $g_2(r)$, $S(k > K)$, and the τ order metric (which measures the degree of translational order) in $d = 2$–8. While we cannot simulate dimensions high enough to show complete decorrelation, we show a loss of higher-order structure that is consistent with both the decorrelation principle [20] and the mean-field theory of hard-sphere liquids and glasses [22,23]. By understanding how structure diminishes in stealthy hyperuniform systems as a function of dimension, we can then begin to understand the role of spatial structure in determining the many novel properties of stealthy hyperuniform systems in the physical dimensions $d = 1$–3 [7,24–45].

The goals of this work are then threefold. First, in Sec. II we give basic definitions and derive the constraints on all stealthy hyperuniform point patterns (both ordered and disordered) imposed by the hard-sphere condition. In Sec. III we use these constraints to confirm that the densest Fourier-space configuration (i.e., the highest value of K for a fixed number density of points) is a Bravais lattice, as stated in Ref. [8]. Then in Sec. IV we discuss disordered stealthy hyperuniform systems and derive their effective Fourier-space packing fraction from the virial theorem. This then allows us to compare to numerical results showing decorrelation in Sec. V. Finally, in Sec. VI we summarize our results and discuss the implications they have on glasses.

II. DEFINITIONS

A Bravais lattice $\Lambda \in \mathbb{R}^d$ is a subgroup consisting of integer linear combinations of vectors constituting a basis for $\mathbb{R}^d$. There are d basis vectors of Λ labeled $\mathbf{a}_i$, and every point on the lattice can be specified as

$$\mathbf{p} = \sum_{i=1}^{d} n_i \mathbf{a}_i, \tag{1}$$

where $n_i \in \mathbb{Z}$. In lattices, space can be divided into identical regions F called fundamental cells that each contain a single point $\mathbf{p}$. The volume of F is denoted by v_F. Bravais lattices are often simply referred to as lattices in mathematics, so to avoid confusion, we will adopt this terminology henceforth. Periodic structures with an m-particle basis will then be denoted as crystals, noting that a lattice is simply a crystal with $m = 1$.

Every lattice has a dual lattice Λ^*, whose points are defined such that that if $\mathbf{p} \in \Lambda$ and $\mathbf{q} \in \Lambda^*$, then $\mathbf{p} \cdot \mathbf{q} = 2\pi m$, where $m \in \mathbb{Z}$. The dual fundamental cell F^* has a volume $v_{F^*} = (2\pi)^d / v_F$ such that the number densities of the lattice ρ_Λ and its dual ρ_{Λ^*} are related as

$$\rho_\Lambda \rho_{\Lambda^*} = \frac{1}{(2\pi)^d}. \tag{2}$$

While the concept of a dual lattice can be formally extended in some cases to crystals [46,47], most crystals with $m > 1$ do not have a formal dual, and Eq. (2) cannot generally be extended to them.

In addition to lattices and crystals, we consider disordered point patterns consisting of N-point particles in $\mathbb{R}^d$ embedded in periodic boxes F with volume v_F with positions $\mathbf{r}_j$. The structure factor for any of the aforementioned individual systems is given by

$$S(\mathbf{k}, \mathbf{r}^N) = \frac{|\tilde{n}(\mathbf{k}, \mathbf{r}^N)|^2}{N}, \tag{3}$$

where $\mathbf{k}$ is a nonzero dual lattice vector of F, $\mathbf{r}^N$ denotes the positions of all N particles, and $\tilde{n}(\mathbf{k}, \mathbf{r}^N)$ is the complex collective coordinate of the wave vector $\mathbf{k}$ given by

$$\tilde{n}(\mathbf{k}, \mathbf{r}^N) = \sum_{j=1}^{N} \exp(-i\mathbf{k} \cdot \mathbf{r}_j). \tag{4}$$

Disordered stealthy hyperuniform systems can be obtained through the collective coordinate procedure [7,9,48–51], which searches for a global minimum (ground state) of a potential related to $S(\mathbf{k}, \mathbf{r}^N)$ via numerical minimization. This potential energy can be derived as [50]

$$\Phi(\mathbf{r}^N) = \frac{N}{2v_F}\left(\sum_{0<k\leqslant K} \tilde{v}(\mathbf{k}) S(\mathbf{k}, \mathbf{r}^N) - \sum_{0<k\leqslant K} \tilde{v}(\mathbf{k})\right), \tag{5}$$

where $v(\mathbf{r})$ is a positive, bounded, and integrable function with compact support over the interval $0 < k < K$ whose Fourier transform $\tilde{v}(\mathbf{k})$ exists. In practice, because the second term is a potential-dependent constant independent of the positions of the particles, it is dropped, and a disordered stealthy hyperuniform point pattern is then given by $\Phi(\mathbf{r}^N) = 0$. While numerical simulations cannot reach this strict bound, they are able to achieve values of Φ which are indistinguishable from zero [52] to within double [9,48–50] or double-double precision [7]. To simplify notation, the dependence of the structure factor on $\mathbf{r}^N$ will be suppressed throughout this work, instead referring to $S(\mathbf{k})$.

While stealthy hyperuniform systems are characterized by the linear size of the exclusion region K, it is useful to consider the number of independently constrained wave vectors for which $S(\mathbf{k}) = 0$, labeled M. The total number of independent degrees of freedom in a system of N particles is $(N-1)d$, and thus the fraction of independent degrees of freedom that are constrained, labeled χ, is

$$\chi \equiv \frac{M}{(N-1)d}. \tag{6}$$

The maximum value of χ for any disordered system [53] is $\chi = \frac{1}{2}$ for $d \geqslant 2$ [8] (note also that $d = 1$ is a special case, which we do not treat here, for which only $\chi < \frac{1}{3}$ are fully disordered; see Ref. [54]). All systems with $\chi > \frac{1}{2}$ are therefore ordered. In addition to crystalline states, the ordered regime contains stacked slider phases [9,51]. Stacked sliders have implicit constraints that necessitate order (like a crystal), but these states do not contain Bragg peaks and are not periodic in real space (see Refs. [9,51] for visual examples).

Following the arguments of Ref. [8], χ can be calculated in the thermodynamic limit by noting that M is simply half the volume of a sphere of radius K in reciprocal space and by

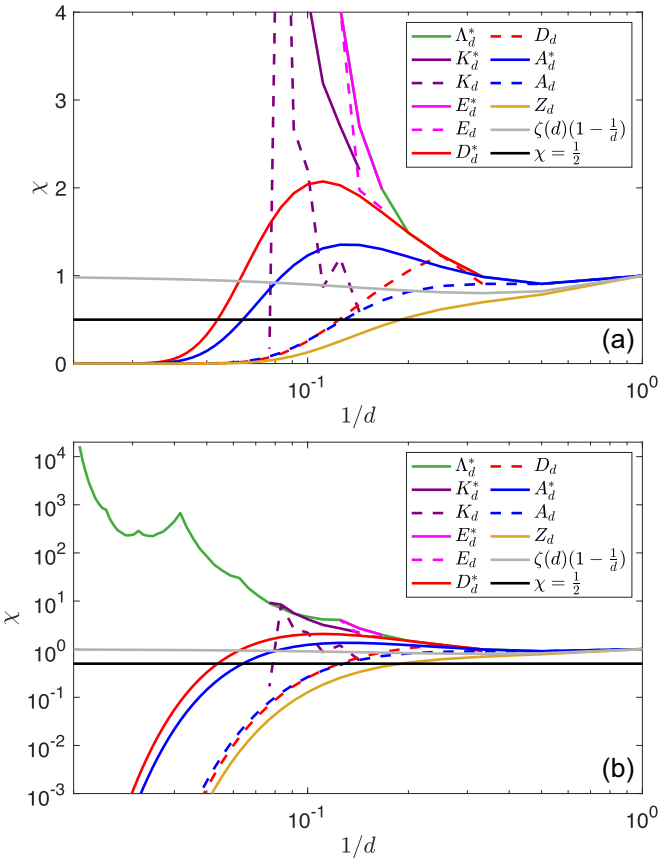

FIG. 2. Plot showing χ for root lattices A_d, D_d, and Z_d; their duals A_d^*, D_d^*, and $Z_d^* = Z_d$; the exceptional root lattices E_d in $d = 6$–8 and their duals E_d^*; K_d and its dual K_d^* in $d = 7$–13; and the duals of the laminated lattices Λ_d in $d = 1$–48. We also show the upper bound for disordered systems, $\chi = \frac{1}{2}$ (gray line), and the lower bound for the densest lattice in any given dimension, $\chi = (1 - \frac{1}{d})\zeta(d)$ (black line) [63], showing that the densest Fourier-space hard-sphere packing in all dimensions is ordered. The same data are plotted with χ in both (a) linear and (b) logarithmic scale.

using Eq. (2) to simplify the resulting equation

$$\chi = \frac{v_d K^d}{2d\rho(2\pi)^d}. \tag{7}$$

Here ρ is the number density of points and v_d is the volume of a d-dimensional sphere of unit radius

$$v_d = \frac{\pi^{d/2}}{\Gamma\left(1 + \frac{d}{2}\right)}. \tag{8}$$

III. DENSEST STEALTHY HYPERUNIFORM CONFIGURATIONS

There are two natural points of interest when discussing χ as an effective packing fraction: (i) the transition point between disordered and ordered systems at $\chi = \frac{1}{2}$ for $d \geqslant 2$ and (ii) the maximum obtainable value of χ in each dimension, which we denote by $\chi_{\max}$. In Ref. [8] it was shown that $\chi_{\max}$ is associated with the lattice that is the dual to the densest lattice in real space. This section is devoted to finding an expression for $\chi_{\max}$ that makes this statement more explicit and that allows the full phase diagram of Fourier-space hard spheres to

be written in any dimension whose densest real-space lattice is known.

To find the maximum value of χ for a given dimension, we first consider the value of χ for a given lattice Λ, labeled χ_Λ. Here we relate the number density of the dual lattice ρ_{Λ^*} to its packing fraction φ_{Λ^*} by assuming spheres of diameter K:

$$\rho_{\Lambda^*} = \frac{2^d \varphi_{\Lambda^*}}{v_d K^d}. \tag{9}$$

Combining this with Eq. (7) yields

$$\chi_\Lambda = \frac{2^d \varphi_{\Lambda^*}}{2d} = \frac{\hat{\varphi}_{\Lambda^*}}{2}. \tag{10}$$

Thus, the numerical value of χ associated with a given lattice is directly related to the packing fraction of its dual lattice in real space. Values of χ_Λ for several standard lattices and their duals in $d = 1$–48 are shown in Fig. 2. Notably, Eq. (10) makes explicit use of the scaling notation used to compare disordered real-space hard spheres across dimensions [20,22,23,55,56]

$$\hat{\varphi} = \frac{2^d \varphi}{d}. \tag{11}$$

This scaling ensures that the minimal jamming packing fraction, the (avoided [57]) dynamical transition, and the onset of Fickian diffusion are all $O(1)$ and smoothly evolve as $d \to \infty$ [58–62]. The appearance of this scaling when considering lattices is a subtle point, which has been noted elsewhere [60,61,63]. Here it will be used to make previous statements about the densest Fourier-space hard-sphere packing more apparent.

From Eq. (10) we define the absolute maximum $\chi_{\max}$ as the maximum value of χ_Λ taken over all crystals Λ in a given dimension,

$$\chi_{\max} \equiv \max_\Lambda(\chi_\Lambda). \tag{12}$$

We have two tools which allow for the calculation of χ_Λ when the maximum packing fraction of the dual (φ_{Λ^*}) is unknown or when the dual does not exist (i.e., in crystals with $m > 1$ or stacked slider phases). The first of these is an application of the stacked slider theorem [51]

$$\chi = \frac{v_d K_m^d}{2d(2\pi)^d \rho_P \rho_Q}, \tag{13}$$

where P and Q refer to lower-dimensional crystals, for which $d_P + d_Q = d$ and $K_m = \min(K_P, K_Q)$. Applying this recursively allows the calculation of $\chi_{\max}$ in all laminated lattices. The second tool is an application of the lemma on additive stealthy systems [8], which states that for a system made additively from m stealthy subsystems with the same value of K, the combined value of χ is

$$\chi = \left(\sum_{i=1}^{m} \chi_i^{-1}\right)^{-1}. \tag{14}$$

Here, because $\chi_i > 0$ for all i, we have that $\chi < \chi_i$ for all i. Thus the value of χ for a crystal with an m-particle basis is lower than that of the lattice with the same unit cell. In Ref. [8] this was used to show that the densest crystal in Fourier space is a lattice. From the construction of Eq. (10) it is then clear that the densest lattice in Fourier space is the dual of the densest lattice in real space, a statement noted in $d = 1$–4 in Ref. [8]. This lattice was also proven to be the unique ground state in any given dimension [64].

Furthermore, it was shown [8] that the densest lattice in Fourier space is more dense than the densest disordered system by logically extending the results of $d = 1$–4. The explicit connection to real-space systems from Eq. (10) allows us to reinforce that proof. While the best lower [16] and upper bounds [17,18] on general sphere packings put the densest packing in the range

$$\max_\Lambda(\hat{\varphi}_\Lambda) \in \left(65\,963, \frac{2^{0.401d}}{d}\right), \tag{15}$$

as $d \to \infty$, a much weaker constructive lower bound is all that is necessary to prove that $\chi_{\max}$ is associated with a lattice. For any given dimension, Ball showed that a lattice Λ_B exists with $\hat{\varphi}_{\Lambda_B} \geqslant 2(1 - \frac{1}{d})\zeta(d)$, where $\zeta(d)$ is the Riemann zeta function [63], and thus

$$\chi_{\max} \geqslant \left(1 - \frac{1}{d}\right)\zeta(d) \tag{16}$$

for $d > 1$. Note that for $d = 1$ where $\zeta(1)$ diverges, $\chi_{\max} = 1$. For positive integers d, $\zeta(d) \to 1^+$ as $d \to \infty$, which converges rather quickly, meaning that $\chi_{\max} > \frac{1}{2}$ in all dimensions.

One caveat, which is clear from Fig. 2, is that while $\chi_{\max} > \frac{1}{2}$ in all dimensions, individual lattices may have $\chi_\Lambda < \frac{1}{2}$ in any dimension, such as Z_d for $d > 5$. Additionally, crystals may have $\chi_\Lambda < \frac{1}{2}$ even in low dimensions, such as kagome ($\chi = 0.3022$) and honeycomb ($\chi = 0.4534$) crystals in $d = 2$ and the pyrochlore ($\chi = 0.2267$) and diamond ($\chi = 0.4534$) crystals in $d = 3$ [8].

IV. MAPPING TO REAL-SPACE DISORDERED SYSTEMS

While we have focused so far on the exclusion region $S(k < K)$, we would like to predict the behavior of the structure factor of disordered stealthy hyperuniform systems outside the exclusion region, i.e., $S(k \geqslant K)$. In Ref. [8], a subset of stealthy hyperuniform systems was identified for which this problem was tractable, namely, entropically favored states (EFSs), which are first thermally equilibrated at a low temperature and then rapidly quenched through energy minimization. The EFSs thus act like equilibrium Fourier-space hard spheres. Following Ref. [8], we use the mapping between a stealthy hyperuniform ensemble with $S(k)$ at an effective packing fraction χ and a real-space hard-sphere ensemble with $g_2^{\mathrm{HS}}(r)$ at real-space packing fraction $\hat{\varphi}$ by

$$S(k, \chi) = g_2^{\mathrm{HS}}(r = k, \hat{\varphi}), \tag{17}$$

where $\chi = b(d)\hat{\varphi}$. Because Eq. (17) is only a statement of two-point correlators, it should only be accurate for small values of χ, though it should be increasingly accurate as d increases and higher-order correlations become trivial due to the decorrelation principle [20]. Whether this mapping is precisely realizable in a given d at any order of approximation is left as an open question.

To first order in $\hat{\varphi}$, the pair-correlation function for equilibrated hard spheres can be written as [65,66]

$$g_2^{\rm HS}(r) = \Theta(r-\sigma)[1+\hat{\varphi}\alpha(r;R)d + \mathcal{O}(\hat{\varphi}^2)], \tag{18}$$

where $\alpha(r;R)$ is the overlap of two spheres of radius R separated by a distance r [65],

$$\alpha(r;R) = \frac{2\Gamma(1+\frac{d}{2})}{\pi^{1/2}\Gamma(\frac{d+1}{2})}\int_0^{\cos^{-1}(r/2R)} \sin^d(\theta)d\theta. \tag{19}$$

The special case $r = R$, which obtains the maximum value of $\alpha(r;R)$, is then

$$\alpha(R;R) = \frac{{}_2F_1\left(\frac{1}{2},\frac{1+d}{2};\frac{3+d}{2};\frac{3}{4}\right)\Gamma\left(1+\frac{d}{2}\right)\left(\frac{3}{4}\right)^{(1+d)/2}}{\pi^{1/2}\Gamma\left(\frac{3+d}{2}\right)}, \tag{20}$$

where ${}_2F_1$ is the ordinary hypergeometric function. In infinite dimensions, $g_2^{\rm HS}(r)$ approaches a step function for all densities [20,61,67], which is reflected in the asymptotic form of the coefficient of $\hat{\varphi}$ at the maximum value $r = R$:

$$\alpha(R;R)d \sim \sqrt{\frac{6d}{\pi}}\left(\frac{3}{4}\right)^{d/2}. \tag{21}$$

As expected, this asymptotes to zero for all values of $\hat{\varphi}$ as $d \to \infty$, and $g_2^{\rm HS}(r)$ approaches a step function.

Using the mapping of Eq. (17), we obtain [68]

$$S(k) = \Theta(k-K)[1+b(d)\chi\alpha(k;K)d + O(\hat{\varphi}^2)]. \tag{22}$$

In Ref. [8] it was argued that $b(d) = [\alpha(K;K)d]^{-1}$, noting a strong fit to $d = 2$ and $d = 3$ data [69]. However, this scaling gives an erroneous result in the prediction for $S(K)$ yielding $S(K) = 1+\chi+O(\chi^2)$. By construction, $S(k)$ should approach a step function as dimension increases, and thus $S(K)$ should approach 1 as $d \to \infty$ for all values of $\chi < 1/2$. In Sec. III we noted that χ could be compared directly to real-space packing fractions in hatted units [see Eq. (11)], suggesting that $b(d) = 1$, and thus

$$S(k) = \Theta(k-K)[1+\chi\alpha(k;K)d + O(\chi^2)]. \tag{23}$$

Figure 3 demonstrates that this achieves the appropriate limit to first order in χ, because $\alpha(K;K)d \to 0$ as $d \to \infty$. Over the densities considered in Ref. [8], the differences between the choices of $b(d) = 1$ and $b(d) = [\alpha(K;K)d]^{-1}$ yield curves which are almost indistinguishable, and thus Eq. (23) fits EFS simulation data well (see the Appendix).

It is of course important to note that the mapping of Eq. (17) does not imply that all real-space hard-sphere properties can be directly transferred to Fourier-space hard spheres. In Eq. (17) the mapping is only made at the two-particle level, which is most relevant at low densities and in high dimensions. We thus expect it to fail when considering highly correlated systems. It is thus unsurprising that the configuration with the maximum effective packing fraction in Fourier space [Eq. (10)] is not what might have been expected using a straightforward substitution $\hat{\varphi} \to \chi$. Similarly, the freezing point for Fourier hard spheres appears to be $\chi = \frac{1}{2}$, while for real-space hard spheres, $\hat{\varphi}_f \sim 1$ in $d = 3$–10 (see Ref. [60] for numerical values) [70].

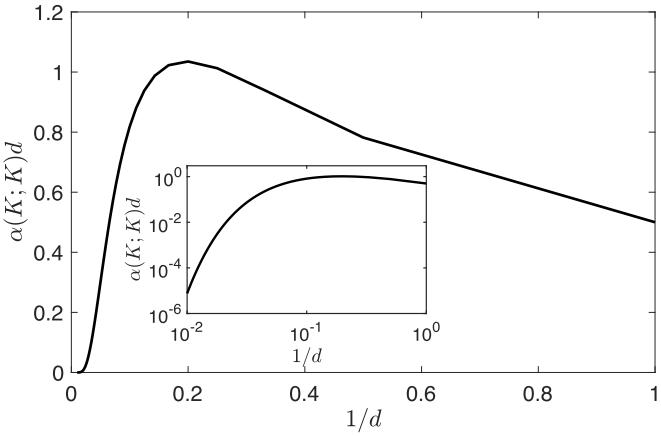

FIG. 3. First-order coefficient in the χ expansion of $S(k)$ for entropically favored states $\alpha(K;K)d$ as a function of dimension. We see that $\alpha(K;K)d \sim O(1)$ for $d \lesssim 20$, but it then rapidly decreases as $d \to \infty$.

V. EVOLUTION OF STRUCTURE IN DISORDERED SYSTEMS

The collective coordinate minimization procedure described in Sec. II can be used to create disordered stealthy hyperuniform systems by minimizing $S(\mathbf{k})$ in the exclusion region. The behavior of the structure factor outside the exclusion region $S(k > K)$ and the pair-correlation function $g_2(\mathbf{r})$ will then depend largely on the initial conditions and the type of minimizer used [50]. While the theory of Ref. [8] gives theoretical predictions for both $g_2(r)$ and $S(k > K)$ in EFSs, these states are difficult to obtain when N is large, and the question of how to create EFSs at large scales is left for future work. We instead focus on states with random initial conditions, equivalent to an infinite-temperature quench (ITQ), and ask whether key features predicted in EFSs remain.

Figure 4 shows ITQ data in $d = 2$–8 for $\chi = 0.1$, 0.2, 0.3, and 0.4 averaged over five systems with $N = 2\times10^5$. In $d = 2$, we see large discrepancies between the theoretical values of $g_2(0)$ and $S(K)$ from EFSs as already noted in Ref. [50] (see Fig. 1 therein) but these differences become negligibly small as dimension increases. For higher values of χ, the nonmonotonicity in $S(k)$ predicted in EFSs are present in ITQ ensembles. However, the oscillations in $S(k)$ at high χ and the spike near $k = K$ present in ITQ systems both decrease as dimension increases, in agreement with the decorrelation principle [20]. We also note an apparent exclusion region forming in $g_2(r)$ for high values of χ, which has been observed elsewhere in large but finite systems [9,50] and exploited to map to packings of nonoverlapping spheres. [26].

In addition to $g_2(r)$ and $S(k)$, we measure the degree of translational order through the order metric τ [8], given by

$$\tau \equiv \frac{1}{D^d}\int_{\mathbb{R}^d}[g_2(\mathbf{r})-1]^2 d\mathbf{r} = \frac{1}{(2\pi D)^d\rho^2}\int_{\mathbb{R}^d}[\langle S(\mathbf{k})\rangle - 1]^2 d\mathbf{k}, \tag{24}$$

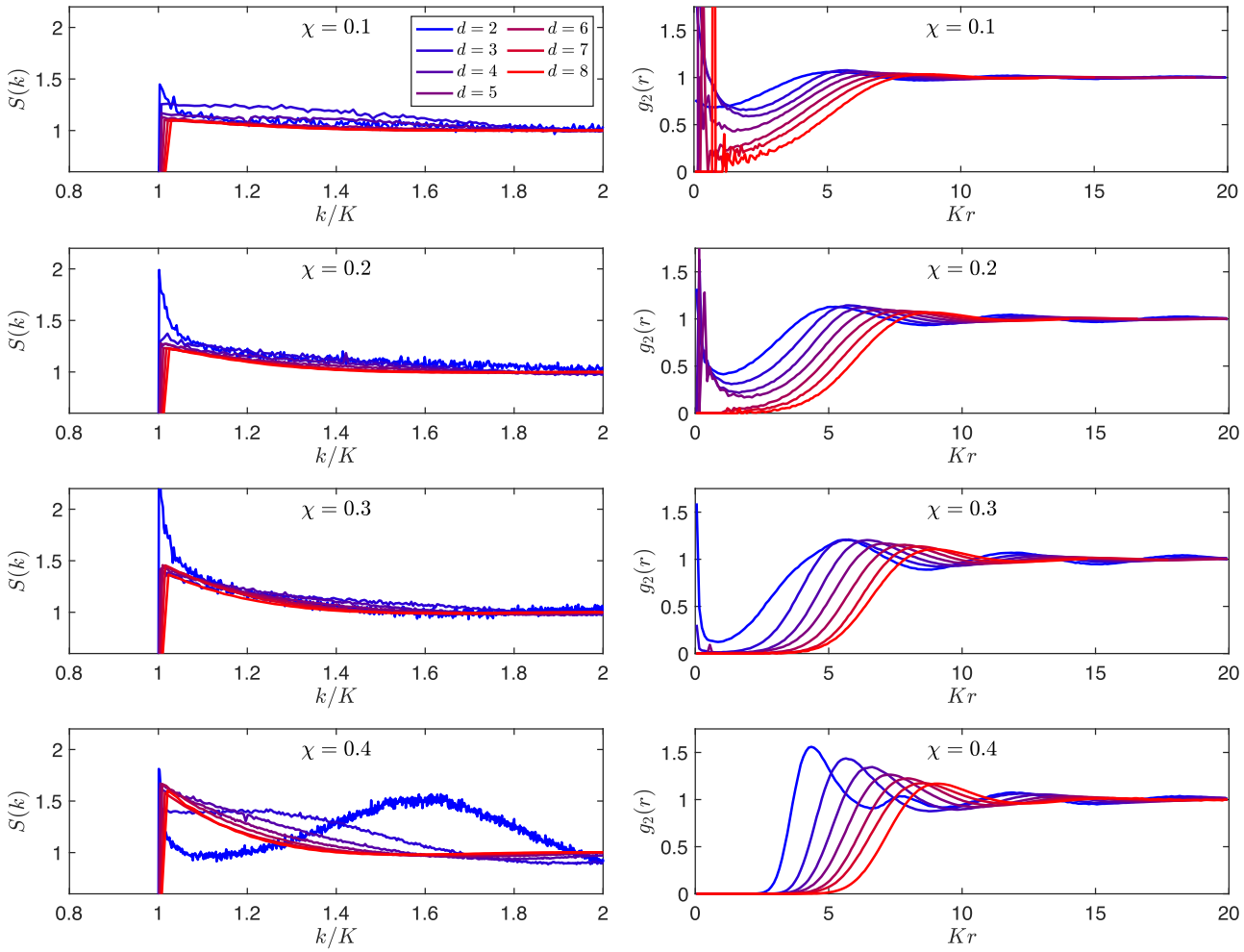

FIG. 4. Plots of $S(k)$ (left) and $g_2(r)$ (right) at fixed χ. As dimension increases, several prominent features in both metrics decrease, namely, the peaks at low values of k and r, respectively, and oscillations in $S(k)$ at high values of χ. As $d \to \infty$, $S(k)$ tends towards a step function for all values of χ; however, the dimensional range shown here is not enough for this trend to be clear, as the first correction to the step function in Eq. (23) is $O(1)$ for $d \lesssim 20$ (see Fig. 3). Instead, the curves appear to collapse towards a common curve as dimension increases. Noise in low-χ high-dimensional $g_2(r)$ data at small values of r is due solely to low sampling.

where angular brackets $\langle \ldots \rangle$ denote an average over configurations and D is a characteristic length, which we take to be $D = K^{-1}$. In an ideal gas $\tau = 0$, and thus τ represents the degree of departure from the fully uncorrelated case. To compare systems across dimension, we define a modified version, labeled $\hat{\tau}$, which for isotropic systems $[g_2(\mathbf{r}) = g_2(r)]$ is

$$\hat{\tau} \equiv \frac{v_d \tau}{4d^2(2\pi)^d} = \frac{K^d v_d^2}{4d(2\pi)^d} \int_0^\infty [g_2(r) - 1]^2 r^{d-1} dr$$
$$= \frac{K^d v_d^2}{4d\rho^2(2\pi)^{2d}} \int_0^\infty [\langle S(k) \rangle - 1]^2 k^{d-1} dk. \tag{25}$$

For EFSs, to first order in χ, this integral can be broken up into three regions using the form of Eq. (23),

$$[S(k) - 1]^2 = \begin{cases} 1 & \text{if } k < K \\ \chi^2 \alpha(k; K)^2 d^2 & \text{if } K \leqslant k \leqslant 2K \\ 0 & \text{if } k > 2K. \end{cases} \tag{26}$$

The integral over the region $k < K$ is trivially χ^2, and the integral over the region $k > 2K$ is trivially zero. The integral over the region $K \leqslant k \leqslant 2K$ can then be reduced to a nondimensional form to become

$$\frac{K^d v_d^2 \chi^2 d}{4\rho^2(2\pi)^{2d}} \int_K^{2K} \alpha(k; K)^2 k^{d-1} dk = \chi^4 d^3 \int_1^2 \alpha(t, 1)^2 t^{d-1} dt$$
$$= c_4(d) \chi^4, \tag{27}$$

where $c_4(d)$ can be calculated numerically. We can thus write

$$\hat{\tau} = \chi^2 + c_4(d)\chi^4 + O(\chi^5). \tag{28}$$

Values of $c_4(d)$ rapidly decrease with dimension above $d \approx 20$ (see Fig. 5), meaning that $\hat{\tau} \to \chi^2$ as $d \to \infty$, which is the result one would get using $S(k) = \Theta(k - K)$. Given that the χ^2 contribution will be common to all stealthy systems, we examine the excess contribution to $\hat{\tau}$ as $\hat{\tau} - \chi^2$.

This can then be compared to the ITQ data (Fig. 6), where we find remarkable functional agreement with the EFS predic-

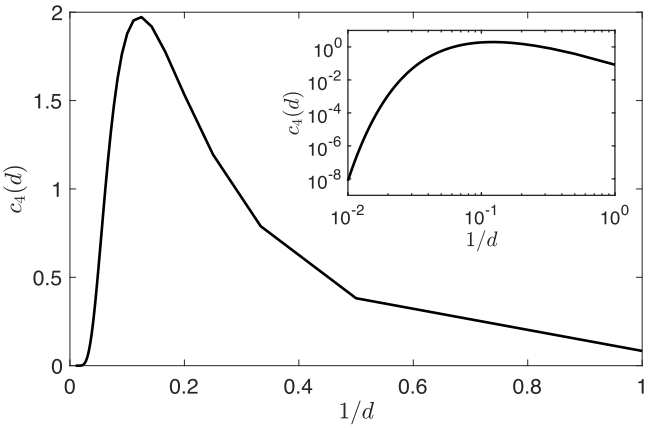

FIG. 5. Coefficient $c_4(d)$ of the χ^4 term in the expansion of $\hat{\tau}$ in Eq. (28) plotted as a function of dimension. While $c_4(d) \sim O(1)$ for $d \lesssim 20$, it then decreases rapidly as $d \to \infty$.

tion as d increases, yielding $\hat{\tau} - \chi^2 \approx \bar{c}\chi^4$ for $d > 4$ with $\bar{c}$ approaching $c_4(d)$ as dimension increases. As noted in Ref. [7], this indicates that, in $d = 2$, the integrated measure of order across length scales is essentially the same between EFSs and ITQ states, despite significant departures in both $S(k)$ and $g_2(r)$, and this is increasingly true as dimension increases.

The decorrelation effects seen in both $S(k)$ and τ indicate that disordered systems are also generally easier to find as dimension increases. This is borne out through the collective coordinate minimization procedure, which becomes significantly faster in higher dimensions and which always finds a global minimum. This also strongly indicates that ground states will continue to exist for all $\chi < \frac{1}{2}$ as $d \to \infty$.

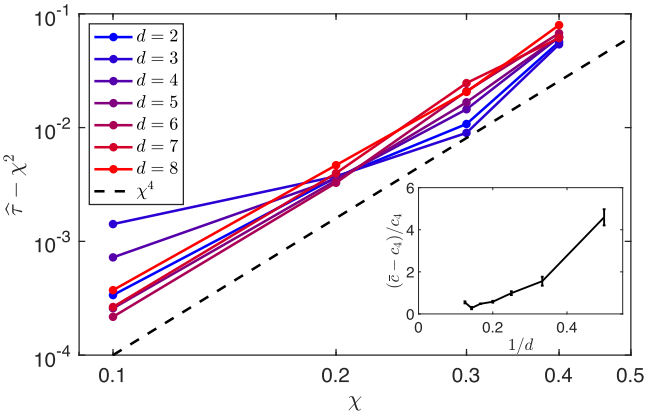

FIG. 6. Excess $\hat{\tau}$ order metric $\hat{\tau} - \chi^2$ as a function of both d and χ from the $N = 2 \times 10^5$ infinite-temperature quench data (circles). For $d > 4$, the ITQ data match the functional form of the entropically favored state prediction $\hat{\tau} - \chi^2 \approx \bar{c}\chi^4$ (black dashed line). Lines between points are kept as a guide to the eye. The prefactor to the quartic term $\bar{c}$ also approaches $c_4(d)$ as d increases, as evidenced in the inset, which shows the relative error of $\bar{c}$.

VI. CONCLUSION

By elaborating on the analogy of stealthy hyperuniform points patterns as hard spheres in Fourier space, we have made several connections that allow insight into real-space packing problems. While the full phase diagram for real-space hard spheres is contested in high dimensions [21], the case for Fourier hard spheres is far simpler. In all dimensions $d \geqslant 2$, systems with $\chi < \frac{1}{2}$ are generically disordered ground states, with crystalline and stacked slider phases comprising a zero-measure set. For $\chi > \frac{1}{2}$, only crystalline and stacked slider phases are allowed, and we have derived a set of relations which clarify that the densest Fourier hard-sphere packing in any dimension is the dual to the densest Bravais lattice in real space, as previously shown [8]. In $d = 1$–8, the densest known Fourier-space hard-sphere packing happens to correspond to the best known solution to the quantizer problem [11], though this correspondence is notably broken in $d = 9$ and 10 [72].

Furthermore, features in $S(k > K)$, $g_2(r)$, and the τ order metric of disordered stealthy hyperuniform states decorrelate as dimension increases, implying that higher-order correlations become trivial. This implies that disordered stealthy hyperuniform systems should be reconcilable with the infinite-dimensional mean-field theory of glasses [22,23], wherein all pair interactions between spheres are completely decorrelated. In infinite dimensions, the EFSs become the full Fourier-space equivalent of real-space equilibrium hard spheres, whose dynamics and phase behavior are well understood within the mean-field theory. A full investigation of this mapping is therefore within reach.

ACKNOWLEDGMENTS

The research was sponsored by the Army Research Office and was accomplished under Cooperative Agreement No. W911NF-22-2-0103. Simulations were performed on computational resources managed and supported by the Princeton Institute for Computational Science and Engineering.

APPENDIX: COMPARISON OF DENSITY SCALING FACTORS

Here we compare the structure factor of stealthy systems under the EFS ensemble summarized in Eq. (22). In Fig. 7 the two scalings of $b(d)$ noted in Sec. IV are plotted for the χ values considered in Ref. [8] for $d = 3$ point patterns: $\chi = 0.05$, 0.1, and 0.143. In Refs. [8,69], it was argued that $b(d) = 1/\alpha(K;K)d$ because it fit the simulation data. Here we argue that $b(d) = 1$ based on the requirements of the $d \to \infty$ scaling and a strict use of χ as the relevant effective density for stealthy systems. While the prefactors differ dramatically, the curves are nearly indistinguishable over the ranges considered, which led to the erroneous adoption of $b(d) = 1/\alpha(K;K)d$ in the previous work [8].

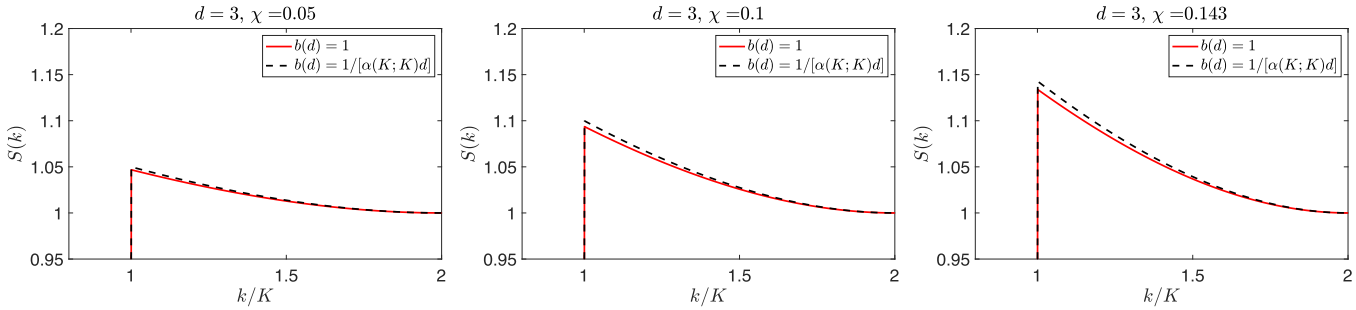

FIG. 7. Comparison of the structure factor for entropically favored states [Eq. (22)] with the previously reported [8] value of $b(d) = 1/\alpha(K;K)d$ and the corrected value $b(d) = 1$ used in this work. Note that the curves are nearly indistinguishable over the range of χ values studied in Ref. [8] and differences between the two curves are smaller than the margin of error for the simulation data contained therein.

[1] S. Torquato and F. H. Stillinger, Local density fluctuations, hyperuniformity, and order metrics, Phys. Rev. E **68**, 041113 (2003).

[2] S. Torquato, Hyperuniform states of matter, Phys. Rep. **745**, 1 (2018).

[3] M. Florescu, S. Torquato, and P. J. Steinhardt, Designer disordered materials with large, complete photonic band gaps, Proc. Natl. Acad. Sci. USA **106**, 20658 (2009).

[4] A. R. McGurn, K. T. Christensen, F. M. Mueller, and A. A. Maradudin, Anderson localization in one-dimensional randomly disordered optical systems that are periodic on average, Phys. Rev. B **47**, 13120 (1993).

[5] C. M. Aegerter and G. Maret, Coherent backscattering and Anderson localization of light, in *Progress in Optics* (Elsevier, 2009), Vol. 52, pp. 1–62.

[6] F. Sgrignuoli, S. Torquato, and L. Dal Negro, Subdiffusive wave transport and weak localization transition in three-dimensional stealthy hyperuniform disordered systems, Phys. Rev. B **105**, 064204 (2022).

[7] P. K. Morse, J. Kim, P. J. Steinhardt, and S. Torquato, Generating large disordered stealthy hyperuniform systems with ultrahigh accuracy to determine their physical properties, Phys. Rev. Res. **5**, 033190 (2023).

[8] S. Torquato, G. Zhang, and F. H. Stillinger, Ensemble theory for stealthy hyperuniform disordered ground states, Phys. Rev. X **5**, 021020 (2015).

[9] O. U. Uche, F. H. Stillinger, and S. Torquato, Constraints on collective density variables: Two dimensions, Phys. Rev. E **70**, 046122 (2004).

[10] J. H. Conway and N. J. A. Sloane, *Sphere Packings, Lattices and Groups*, 2nd ed., Grundlehren Der Mathematischen Wissenschaften (Springer-Verlag, New York, 1993).

[11] S. Torquato, Reformulation of the covering and quantizer problems as ground states of interacting particles, Phys. Rev. E **82**, 056109 (2010).

[12] J.-L. Lagrange, Recherches d'arithmétique, Nouv. Mém. Acad. R. Soc. Belles Lettres Berlin **1773**(5), 265 (1775).

[13] T. C. Hales, A proof of the Kepler conjecture, Ann. Math. Second Ser. **162**, 1065 (2005).

[14] M. S. Viazovska, The sphere packing problem in dimension 8, Ann. Math. Second Ser. **185**, 991 (2017).

[15] H. Cohn, A. Kumar, S. D. Miller, D. Radchenko, and M. Viazovska, The sphere packing problem in dimension 24, Ann. Math. Second Ser. **185**, 1017 (2017).

[16] A. Venkatesh, A note on sphere packings in high dimension, Int. Math. Res. Not. **2013**, 1628 (2013).

[17] G. A. Kabatiansky and V. I. Levenshtein, On bounds for packings on a sphere and in space, Probl. Peredachi Inf. **14**, 3 (1978).

[18] H. Cohn and Y. Zhao, Sphere packing bounds via spherical codes, Duke Math. J. **163**, 1965 (2014).

[19] M. Best, Binary codes with a minimum distance of four (Corresp.), IEEE Trans. Inf. Theory **26**, 738 (1980).

[20] S. Torquato and F. H. Stillinger, New conjectural lower bounds on the optimal density of sphere packings, Exp. Math. **15**, 307 (2006).

[21] P. Charbonneau, P. K. Morse, W. Perkins, and F. Zamponi, Three simple scenarios for high-dimensional sphere packings, Phys. Rev. E **104**, 064612 (2021).

[22] G. Parisi and F. Zamponi, Mean-field theory of hard sphere glasses and jamming, Rev. Mod. Phys. **82**, 789 (2010).

[23] G. Parisi, Pierfrancesco, and Zamponi, Francesco, *Theory of Simple Glasses: Exact Solutions in Infinite Dimensions*, 1st ed. (Cambridge University Press, New York, 2020).

[24] W. Man, M. Florescu, E. P. Williamson, Y. He, S. R. Hashemizad, B. Y. C. Leung, D. R. Liner, S. Torquato, P. M. Chaikin, and P. J. Steinhardt, Isotropic band gaps and freeform waveguides observed in hyperuniform disordered photonic solids, Proc. Natl. Acad. Sci. USA **110**, 15886 (2013).

[25] O. Leseur, R. Pierrat, and R. Carminati, High-density hyperuniform materials can be transparent, Optica **3**, 763 (2016).

[26] G. Zhang, F. H. Stillinger, and S. Torquato, Transport, geometrical, and topological properties of stealthy disordered hyperuniform two-phase systems, J. Chem. Phys. **145**, 244109 (2016).

[27] B.-Y. Wu, X.-Q. Sheng, and Y. Hao, Effective media properties of hyperuniform disordered composite materials, PLoS One **12**, e0185921 (2017).

[28] L. S. Froufe-Pérez, M. Engel, J. J. Sáenz, and F. Scheffold, Band gap formation and Anderson localization in disordered photonic materials with structural correlations, Proc. Natl. Acad. Sci. USA **114**, 9570 (2017).

[29] G. Gkantzounis, T. Amoah, and M. Florescu, Hyperuniform disordered phononic structures, Phys. Rev. B **95**, 094120 (2017).

[30] D. Chen and S. Torquato, Designing disordered hyperuniform two-phase materials with novel physical properties, Acta Mater. **142**, 152 (2018).

[31] S. Torquato and D. Chen, Multifunctional hyperuniform cellular networks: Optimality, anisotropy and disorder, Multifunct. Mater. **1**, 015001 (2018).

[32] S. Gorsky, W. A. Britton, Y. Chen, J. Montaner, A. Lenef, M. Raukas, and L. Dal Negro, Engineered hyperuniformity for directional light extraction, APL Photonics **4**, 110801 (2019).

[33] V. Romero-García, N. Lamothe, G. Theocharis, O. Richoux, and L. M. García-Raffi, Stealth acoustic materials, Phys. Rev. Appl. **11**, 054076 (2019).

[34] A. Rohfritsch, J.-M. Conoir, T. Valier-Brasier, and R. Marchiano, Impact of particle size and multiple scattering on the propagation of waves in stealthy-hyperuniform media, Phys. Rev. E **102**, 053001 (2020).

[35] A. Sheremet, R. Pierrat, and R. Carminati, Absorption of scalar waves in correlated disordered media and its maximization using stealth hyperuniformity, Phys. Rev. A **101**, 053829 (2020).

[36] J. Kim and S. Torquato, Multifunctional composites for elastic and electromagnetic wave propagation, Proc. Natl. Acad. Sci. USA **117**, 8764 (2020).

[37] V. Romero-García, É. Chéron, S. Kuznetsova, J.-P. Groby, S. Félix, V. Pagneux, and L. M. García-Raffi, Wave transport in 1D stealthy hyperuniform phononic materials made of non-resonant and resonant scatterers, APL Mater. **9**, 101101 (2021).

[38] S. Yu, C.-W. Qiu, Y. Chong, S. Torquato, and N. Park, Engineered disorder in photonics, Nat. Rev. Mater. **6**, 226 (2021).

[39] É. Chéron, S. Félix, J.-P. Groby, V. Pagneux, and V. Romero-García, Wave transport in stealth hyperuniform materials: The diffusive regime and beyond, Appl. Phys. Lett. **121**, 061702 (2022).

[40] M. A. Klatt, P. J. Steinhardt, and S. Torquato, Wave propagation and band tails of two-dimensional disordered systems in the thermodynamic limit, Proc. Natl. Acad. Sci. USA **119**, e2213633119 (2022).

[41] N. Tavakoli, R. Spalding, A. Lambertz, P. Koppejan, G. Gkantzounis, C. Wan, R. Röhrich, E. Kontoleta, A. F. Koenderink, R. Sapienza, M. Florescu, and E. Alarcon-Llado, Over 65% sunlight absorption in a 1 μm Si slab with hyperuniform texture, ACS Photonics **9**, 1206 (2022).

[42] N. Granchi, R. Spalding, M. Lodde, M. Petruzzella, F. W. Otten, A. Fiore, F. Intonti, R. Sapienza, M. Florescu, and M. Gurioli, Near-field investigation of luminescent hyperuniform disordered materials, Adv. Opt. Mater. **10**, 2102565 (2022).

[43] J. Kim and S. Torquato, Effective electromagnetic wave properties of disordered stealthy hyperuniform layered media beyond the quasistatic regime, Optica **10**, 965 (2023).

[44] J. Kim and S. Torquato, Extraordinary optical and transport properties of disordered stealthy hyperuniform two-phase media, J. Phys. Condens. Matter **36**, 225701 (2024).

[45] J. Kim and S. Torquato, Theoretical prediction of the effective dynamic dielectric constant of disordered hyperuniform anisotropic composites beyond the long-wavelength regime [Invited], Opt. Mater. Express **14**, 194 (2024).

[46] H. Cohn, A. Kumar, and A. Schürmann, Ground states and formal duality relations in the Gaussian core model, Phys. Rev. E **80**, 061116 (2009).

[47] H. Cohn, A. Kumar, C. Reiher, and A. Schürmann, Formal duality and generalizations of the Poisson summation formula, in *Discrete Geometry and Algebraic Combinatorics*, Contemporary Mathematics Vol. 625, edited by A. Barg and O. Musin (American Mathematical Society, Providence, Rhode Island, 2014).

[48] O. U. Uche, S. Torquato, and F. H. Stillinger, Collective coordinate control of density distributions, Phys. Rev. E **74**, 031104 (2006).

[49] R. D. Batten, F. H. Stillinger, and S. Torquato, Classical disordered ground states: Super-ideal gases and stealth and equi-luminous materials, J. Appl. Phys. **104**, 033504 (2008).

[50] G. Zhang, F. H. Stillinger, and S. Torquato, Ground states of stealthy hyperuniform potentials: I. Entropically favored configurations, Phys. Rev. E **92**, 022119 (2015).

[51] G. Zhang, F. H. Stillinger, and S. Torquato, Ground states of stealthy hyperuniform potentials. II. Stacked-slider phases, Phys. Rev. E **92**, 022120 (2015).

[52] The precise value that Φ achieves will depend on N, d, K, and $\tilde{v}(\mathbf{k})$.

[53] The value $\chi = \frac{1}{2}$ comes from the constraint that both the real and the imaginary components of $\tilde{n}(\mathbf{k})$ must be zero in order for $S(\mathbf{k}) = 0$.

[54] Y. Fan, J. K. Percus, D. K. Stillinger, and F. H. Stillinger, Constraints on collective density variables: One dimension, Phys. Rev. A **44**, 2394 (1991).

[55] S. Torquato and F. H. Stillinger, Controlling the short-range order and packing densities of many-particle systems, J. Phys. Chem. B **106**, 8354 (2002).

[56] M. Skoge, A. Donev, F. H. Stillinger, and S. Torquato, Packing hyperspheres in high-dimensional Euclidean spaces, Phys. Rev. E **74**, 041127 (2006).

[57] P. Charbonneau, J. Kurchan, G. Parisi, P. Urbani, and F. Zamponi, Glass and jamming transitions: From exact results to finite-dimensional descriptions, Annu. Rev. Condens. Matter Phys. **8**, 265 (2017).

[58] P. K. Morse and P. Charbonneau, Amorphous packings of spheres, in *Packing Problems in Soft Matter Physics*, edited by H.-K. Chan, S. Hutzler, A. Mughal, C. S. O'Hern, Y. Wang, and D. Weaire (Royal Society of Chemistry, Cambridge, 2025).

[59] M. Mangeat and F. Zamponi, Quantitative approximation schemes for glasses, Phys. Rev. E **93**, 012609 (2016).

[60] P. Charbonneau, C. M. Gish, R. S. Hoy, and P. K. Morse, Thermodynamic stability of hard sphere crystals in dimensions 3 through 10, Eur. Phys. J. E **44**, 101 (2021).

[61] P. Charbonneau, Y. Hu, J. Kundu, and P. K. Morse, The dimensional evolution of structure and dynamics in hard sphere liquids, J. Chem. Phys. **156**, 134502 (2022).

[62] P. Charbonneau and P. K. Morse, Jamming, relaxation, and memory in a minimally structured glass former, Phys. Rev. E **108**, 054102 (2023).

[63] K. Ball, A lower bound for the optimal density of lattice packings, Int. Math. Res. Not. **1992**, 217 (1992).

[64] S. Torquato and F. H. Stillinger, New duality relations for classical ground states, Phys. Rev. Lett. **100**, 020602 (2008).

[65] S. Torquato, Effect of dimensionality on the continuum percolation of overlapping hyperspheres and hypercubes, J. Chem. Phys. **136**, 054106 (2012).

[66] J.-P. Hansen and I. McDonald, *Theory of Simple Liquids: With Applications to Soft Matter*, 4th ed. (Academic Press, Amsterdam, 2013).

[67] H. L. Frisch, N. Rivier, and D. Wyler, Classical hard-sphere fluid in infinitely many dimensions, Phys. Rev. Lett. **54**, 2061 (1985).

[68] There is a trivial error in the argument of $\Theta(x)$ and a sign error in the second term of the corresponding equation [Eq. (77)] in Ref. [8], which are corrected here.

[69] In comparing with Ref. [8], we have rescaled the definition of $b(d)$ to simplify the equations.

[70] This approximation of the freezing point may break down as $d \to \infty$. In this limit, it has been conjectured that $\hat{\varphi}_{\rm f} \in (0.144, \ln d)$ [21,71], which includes a diverging value of $\hat{\varphi}_{\rm f}$.

[71] M. Jenssen, F. Joos, and W. Perkins, On the hard sphere model and sphere packings in high dimensions, Forum Math. Sigma **7**, e1 (2019).

[72] E. Agrell and T. Eriksson, Optimization of lattices for quantization, IEEE Trans. Inf. Theory **44**, 1814 (1998).